Everest Advances in Science and Technology (EAST) Vol. 2, No. 1, 2026 (Special Issue)
ISSN: 3102-0410 (Print), 3102-0429 (Online)
DOI: https://doi.org/10.3126/east.v2i2.99472

FEM-Based Parametric Optimization for Driven Soil Nail Systems: Development of Performance-Based Design Charts for Slope Stability and Deformation Control

RAM C. TIWARI[1], AANCHAL TIWARI[1], PRABHAT K. JHA[2], NIRAJ CHAPAGAIN[1], SAMYAK SHRESTHA[1], PRASANT BIST[1], MAHESH KHANAL[1], MOHAMMAD MIYA[1], MANOJ MUKHIYA[1], AAYAM TIWARI[3*]

Abstract. The current study uses a database-driven optimization approach employing FEM analysis in PLAXIS 2D based on the Mohr-Coulomb constitutive model. An automation workflow in Python created 38,880 numerical simulations, among which 17,587 met the geometry and performance criteria. Based on the resulting database, it is possible to assess the effect of the major design parameters on slope stability, deformations, and reinforcement requirement, thus creating design charts for practical engineering purposes. A 30% nail length increase resulted in 10% higher FOS and 12% lower displacement. On the other hand, a 30% increase in backfill angle decreased FOS and increased displacement by 40–45%. At the same time, a 30% increase in face angle did not influence FOS (+/-1%) while decreasing displacement up to 14%. Face angle increase from 0° to 10° led to an increase of the maximum excavation depth from 6 m to 10 m due to reduction of lateral earth pressure and better interaction between the wall and soils. Excavation depth increase by 30% decreased FOS by 10% and displacement by 120%, thus determining the main design parameter. Despite the fact that deeper excavation depths required much larger nails and linearly growing spacing, inclined walls needed much smaller reinforcement increase. About 1,100 models were constrained by deformation criteria while only 350 were controlled by FOS criteria, indicating that deformations were controlling design optimization in most cases. The proposed database and design charts provide the basis for optimized soil-nailed excavation system design.

Keywords: Driven soil nailing; Finite Element Method, Parametric optimization, factor of Safety (FOS), Slope deformation, Design charts

[1] Institute of Engineering, Pulchowk Campus, Tribhuvan University, Lalitpur, Nepal

[2] Ministry of Physical Infrastructure and Transport (MoPIT), Government of Nepal

[3] Advanced College of Engineering and Management, Kathmandu, Nepal

E-mail: aayam2005@gmail.com

* Corresponding author

Manuscript received: 24 March 2026; Revised: 15 June 2026; Accepted: 11 July 2026.

1. INTRODUCTION

Structures that retain play an important role in civil engineering infrastructure to stabilize earth materials and ensure the stability of roads, bridges, and buildings [1]. The use of retaining structures improves the structural stability of soil mass through active measures like piles, buttresses, and prestressed anchors or by using passive methods such as reinforced earth and soil nailing. Soil nailing is a process which is usually employed for strengthening soils. This process was developed out of the "New Austrian Tunneling Method" and is a globally accepted method of stabilizing slopes and repairing excavation sites [2, 3].

Among stabilization techniques, driven soil nailing is increasingly favored due to its ease of implementation. Unlike traditional "drill-and-grout" methods, driven soil nailing utilizes lightweight equipment to install slender reinforcing members directly into the soil mass [4]. This approach offers several logistical advantages: it minimizes traffic disruption, has a smaller environmental footprint, and allows for both "top-down" and "bottom-up" construction according to site geometry. Because the equipment is portable, it is uniquely suited for remote locations where mobilizing heavy drilling rigs is impractical. Furthermore, these structures are inherently flexible, allowing them to accommodate large settlements and perform reliably during seismic events [2, 4].

Though the practicality or "ease" of the driven technique is there, there is still a huge difference between field application and standardized engineering design. There is not much research done on the slope stability problem which leads to individualized analysis in which geotechnical engineers have to engage which in most cases are non-standardized and cost prohibitive. In areas of geologically unstable zones where there is high seismicity and tectonic plates are subducting with the speed of 40–50 mm annually, the risk of slope instability is further enhanced due to non-standardized guidelines [5, 6]. The major thrust planes and jointed sedimentary rocks provide deep-seated instability [7, 8] for which there is no guidebook available in the field for determination of nail length, spacing, and inclinations for different cut heights.

With growing infrastructural target of several thousand kilometers of highway connections, it is no longer feasible to go for design on individual project basis [9, 10]. There arises an imminent need for moving towards standardization with respect to performance based templates. This paper provides solution to the stated challenge by developing "Standard Designed Template for Driven Soil Nail Retaining Structure." By employing the use of database oriented FEM optimization technique comprising over 38,000 simulations, this research paper develops a clear set of design templates. These templates will help the practicing engineer in getting the necessary details to control factor of safety and displacement.

2. METHODOLOGY

The methodology adopted in generating the standardized design charts for driven soil nail systems used a thorough numerical approach, which incorporated both international and national codes. The choice of variables was largely influenced by the Standard Specification for Road and Bridge Works [11]. In order to account for the effect of geometry on stability, parametric analyses were conducted by changing the facing angle from 0° to 10°, in 5° increments. Besides that, the excavation depth was considered within the interval of 1–7 m, in 1 m increments. Various guidelines from all over the world were used to determine the benchmark for investigations, design, and monitoring [3, **?**]. The overall methodological approach is shown in Figure 1 below.

2.1. **Pseudo-static Coefficient.** In order to create seismic load conditions that are needed in order to assure long-term structural stability in seismically active zones, pseudo-static analysis was carried out. As per Nepal National Building Code, the value of k_h was taken from 0.2 to 0.4 in steps of 0.05 [12]. This assures the safety of design curves against large earthquake loads.

2.2. **Numerical Analysis.** Numerical modeling of soil nails has been performed in the computer package Plaxis 2D v20, using 15 noded triangular finite elements for obtaining highly accurate solution under plane strain condition [13]. Although there are many advanced soil models available in Plaxis, in this paper, the Mohr-Coulomb (MC) soil model was considered. The selected model is a linear-elastic and perfectly plastic soil model and is considered efficient because of the findings in earlier studies of soil nail walls [**?**]. The model needs five basic parameters for the numerical analysis, which are shown in Table I, making sure that the design charts can be prepared with assumed soil parameters. Table II provides details of the geometric parameters and the ranges of testing that have been considered in this work, which includes excavation depth, wall batter, facing thickness, nail angle, spacing, and length to depth ratio.

The Mohr-Coulomb (MC) material model was implemented while designing template. This is quick computationally, it is a simplification of reality - particularly in regard to its inability to take into account the effects of strain hardening, progressive failure, and non-Newtonian response. Following conclusions can be drawn while implementing these charts in the field: (1) the design charts can be applied to sites where soil response may be adequately modeled with the MC model - mainly stiff to medium-stiff cohesive and cohesionless soils experiencing small deformations; (2) validation of the design charts with particular soil modeling and, if required, use of more complex constitutive models in a site-specific manner is strongly advised before using the charts for the design; and (3) the design charts cannot be used for soft clays, highly plastic soils, and soils prone to creep and liquefaction without any modification.

TABLE 1. Parameter Required for Mohr Coulomb Analysis

Symbol	**Description**	**Unit**
E	Young's Modulus	[kN/m^2]
ν	Poisson's ratio	[-]
c	Cohesion	[kN/m^2]
ϕ	Friction angle	[°]
ψ	Dilatancy angle	[°]

TABLE 2. Geometric Parameters

Geometric Parameters	**Testing Ranges / Values**	**Units**
Side Slope/Cut Slope Excavation Depth	2,4,6,8,10	meter (m)
Facing Angle (Wall batter)	0,5,10	Degree (°)
Facing Plate Thickness	100–200	millimeter (mm)
Nail Inclination	15	Degree (°)
Nail Spacing	0.5,0.6,0.7,0.8,0.9,1.0,1.1,1.2	meter (m)
Nail Length/Excavation depth	0.4–1.2	meter/meter

Plane strain requires that the three-dimensional, cylindrical soil nail elements are transformed into a two-dimensional element for modeling. Even though other research works have used geogrids as soil nails, this study uses plates as elements for modeling soil nails numerically. Plates differ from geogrids in that they can consider both axial stiffness and bending stiffness of the reinforcement [14]. The importance of considering soil nails as plates in order to capture these two stiffness properties has been emphasized by Singh and Babu [14].

In order to model nail elements using plate elements, the axial stiffness (EA) and flexural rigidity (EI) must be determined. Also for grouted nails, the equivalent modulus of elasticity (E_{eq}) needs

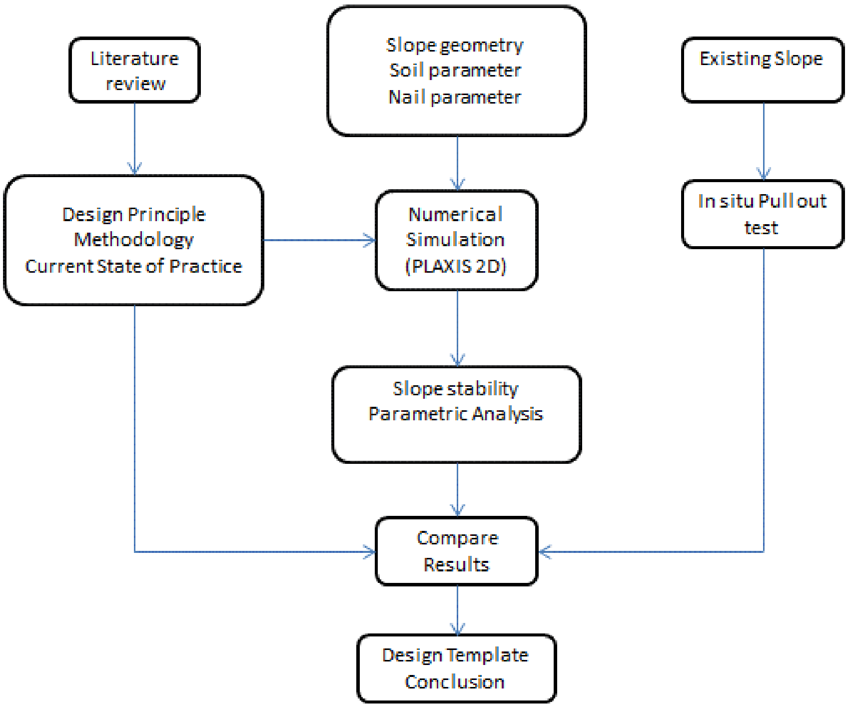

FIGURE 1. Methodological Framework.

to be computed for axial stiffness and flexural rigidity since the elastic stiffness of the grout and nail can be considered. Equation (1) shows the expression for determining equation.

$$E_{eq} = \frac{E_n A_n + E_g A_g}{A} \tag{1}$$

Where: E_n = Modulus of elasticity of nail, A_n = Area of the Nail, d = Diameter of Nail, A = Cross-section area of the grouted hole ($A = 0.25\pi D_{DH}^2$), E_g = Modulus of elasticity of grout, A_g = Cross-sectional area of the grout ($A_g = A - A_n$).

Now Axial Stiffness and Bending stiffness can be calculated according to equations (2) and (3):

$$EA = \text{Axial stiffness [kN/m]} \tag{2}$$

$$EI = \text{Bending stiffness [kNm}^2\text{/m]} \tag{3}$$

Where: S_h = Spacing of the Nail.

Figure 2 illustrates the characteristic deformation of a soil nail wall as it transitions from its initial configuration to a deformed pattern. As excavation height (H) increases, the wall undergoes lateral (δ_h) and vertical (δ_v) displacements, creating a zone of influence (D_{DEF}) that may affect nearby structures. This model, modified after Byrne et al. [15], is essential for quantifying the SSI effect and verifying that nail length (L) and face inclination (α) effectively limit ground movement.

Skin-Driven Stability of Soil Nails depends mainly on skin friction, which is analyzed through embedded beam rows using bond strength according to FHWA standards [?]. For incorporating

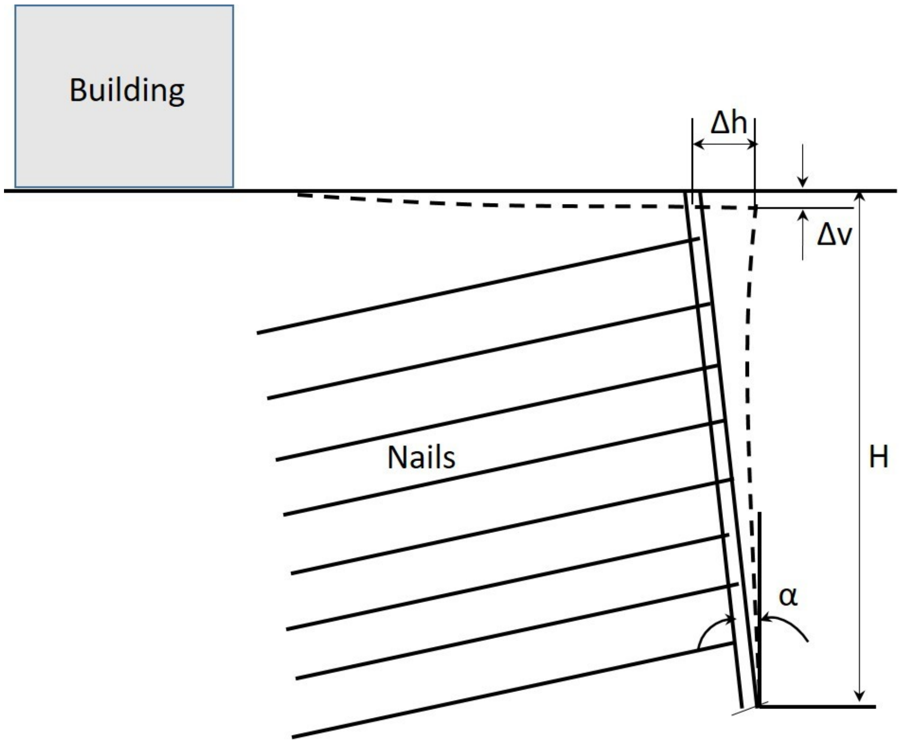

Figure 2. Deformation of the Soil Nail Wall (modified after Byrne et al. [15]).

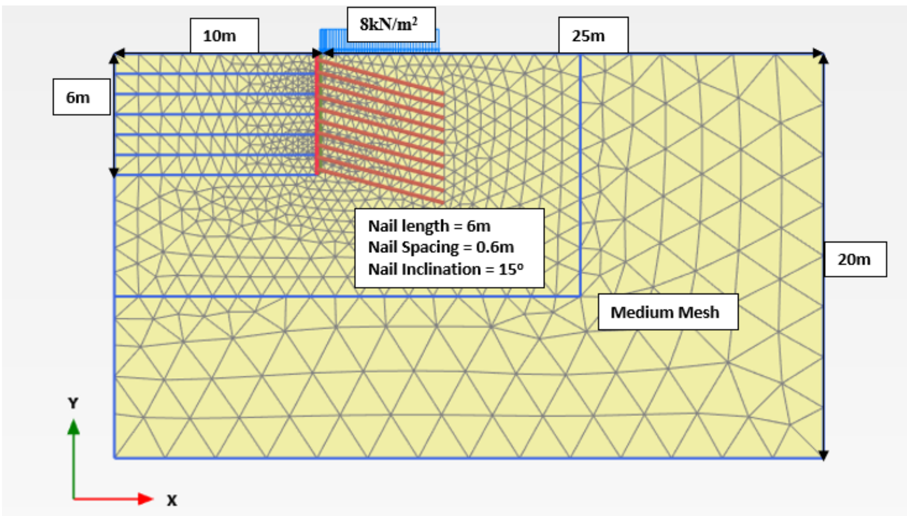

Figure 3. Standard Model Used for Parametric Analysis of Driven Nail.

construction loads, an 8 kN/m^2 surcharge is applied along a 8 m distance from the toe of the retaining wall. The model considers a fine mesh around the nails, with horizontal and full fixing conditions at the lateral and bottom boundary respectively. As illustrated in Figure 3, the simulation follows field procedures consisting of K_0 stress generation, stage-wise plastic analyses and FOS assessment.

Global Factor of Safety is calculated at the end of simulation process while factor of safety is also estimated at some certain stages during the simulation process. Deformation of the lateral displacement of the wall caused by excavation operations is measured at the top of the wall.

In the case of calculation of plastic type, the maximum number of steps used in the calculation is 1000 while the tolerance of error is 0.01. The maximum number of iterations for the calculation is 60. In the case of calculation of safety type, the maximum number of steps used in the calculation is 100 while the tolerance of error is 0.01 and. The maximum number of iterations for the calculation is 60.

2.3. **Parametric Analysis.** Parametric analysis evaluates the influence of nail length, spacing, inclination, and diameter on the Factor of Safety (FOS) and deformation by varying each independently. Geometrical sensitivity is subsequently assessed by adjusting the vertical facing angle and excavation depth. While back-slope variation is considered for drill-and-grout systems, it is excluded for driven nails as they are limited to a 7m maximum height. Following these analyses, optimized configurations are subjected to pseudo-static seismic evaluation using coefficients prescribed by NBC 105: 2020 [**?**].

In this research, out of a total of 38,880 simulations, these were created via a Python-based combinatorial automated simulation platform, including the following parameters: five levels of excavation depth (2, 4, 6, 8, 10 m); three levels of facing angle (0°, 5°, 10°); nine levels of nail length-to-depth ratio (0.4 to 1.2); eight levels of nail spacing (0.5 to 1.2 m); five levels of pseudo-static seismic coefficient (0.2 to 0.4); and twelve soil profiles according to the combinations of cohesion and friction angle. In total, 17,587 simulations passed the criteria for validity (for example, physical admissibility of nail placement) and performance (minimum factor of safety (FOS) = 1.5 and maximum deformation threshold). The criteria of selection, as well as reasons for exclusion of the other models, are now presented clearly.

3. RESULTS AND DISCUSSIONS

The development of these design charts provides a standardized framework for driven soil nail systems, integrating nail geometry, soil properties, and seismic loading into a single performance-based tool. By simplifying complex numerical results, these charts enable field engineers to achieve structural longevity while minimizing time and construction costs. Verification through scaled physical modeling and inclinometer monitoring further ensures that these designs effectively manage the SSI effect and structural deformation.

3.1. **Preparation of Design Charts.** The standardized charts are categorized into twelve distinct soil profiles based on their cohesion (c) and internal friction angle (ϕ) properties. These classifications focus on varying degrees of plasticity and soil consistency to cover the diverse subgrade conditions encountered in the field:

TABLE 3. Design charts according to soil types.

No.	Soil Classification	Primary Constituent	Design Charts
1	Soft, Medium, and Stiff slightly plastic loam	Silt	3*3
2	Soft, Medium, and Stiff low plastic loam	Silt	3*3
3	Soft, Medium, and Stiff low plastic loam	Clay	3*3
4	Medium and Stiff high plastic loam	Clay	3*3

Each chart provides optimized nail configurations (length, spacing, and inclination) tailored to these specific soil categories. This allows for a rapid transition from site investigation to design without the necessity for project-specific FEM modeling for every cut slope, provided the site parameters fall within these established categories.

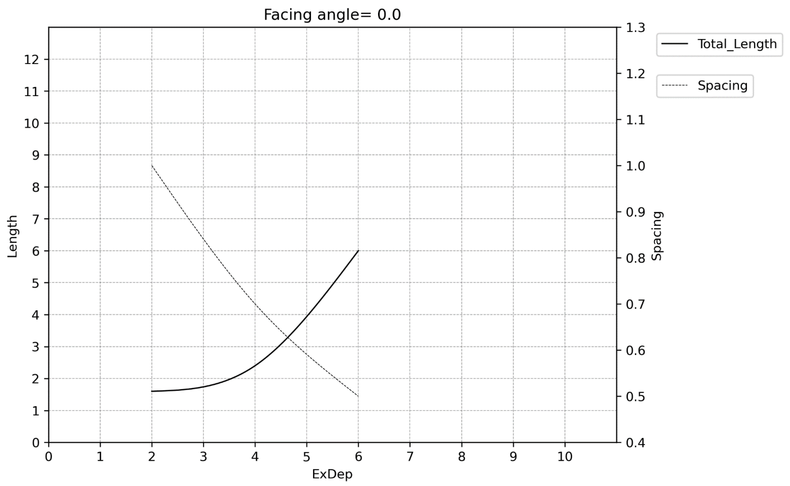

FIGURE 4. For soft slightly plastic loam soil (major quantity: silt, material modelling-Mohr-Coulomb).

The chart in Figure 4 (Top) illustrates the performance-based design requirements for a vertical soil nail wall (facing angle =0.0 degree) as a function of increasing excavation depth. The results reveal a critical inverse relationship between reinforcement geometry and wall height: as the excavation depth progresses from 2 m to 6 m, the required total nail length increases exponentially from approximately 1.6 m to 6 m. Simultaneously, the required spacing between nails must be significantly tightened, decreasing linearly from 1.0 m to 0.5 m to maintain the stability of the soil mass. This trend quantifies the increasing demand on the reinforcement system to manage the SSI effect in deeper cuts, where longer nails and higher installation densities are mandatory to ensure structural integrity and deformation control.

The chart for a 5.0° facing angle illustrates reinforcement trends for excavation depths up to 8 m. As the wall height increases, the Total Length (solid line) grows parabolically from 0.8 m to 6.4 m. To compensate for the increased soil mobilization, the Spacing (dashed line) is reduced from 1.1 m to 0.6 m. This demonstrates that even with a slight inclination, deeper excavations require a substantial increase in both nail length and installation density to effectively manage the SSI effect and ensure structural stability.

For a soil nail wall with a 10.0° facing angle, the design chart illustrates reinforcement requirements for excavation depths extending up to 10 m. The Total Length (solid line) shows a steady, nearly linear increase from 0.8 m to 6.0 m across the excavation range. Simultaneously, the Spacing (dashed line) is reduced from 1.2 m to 0.6 m to provide adequate support as the depth increases. Compared to steeper facing angles, this 10 degrees inclination allows for significantly wider initial nail spacing at shallow depths and maintains a more controlled reinforcement growth rate. However, as the wall approaches a 10 m depth, high-density reinforcement remains essential to mitigate the SSI effect and ensure global stability of the slope.

Based on the above discussions, the following results can be summarized: (i) Effect of nail length on FOS and displacement; 10-11% FOS improvement and 12-13% displacement reduction for a

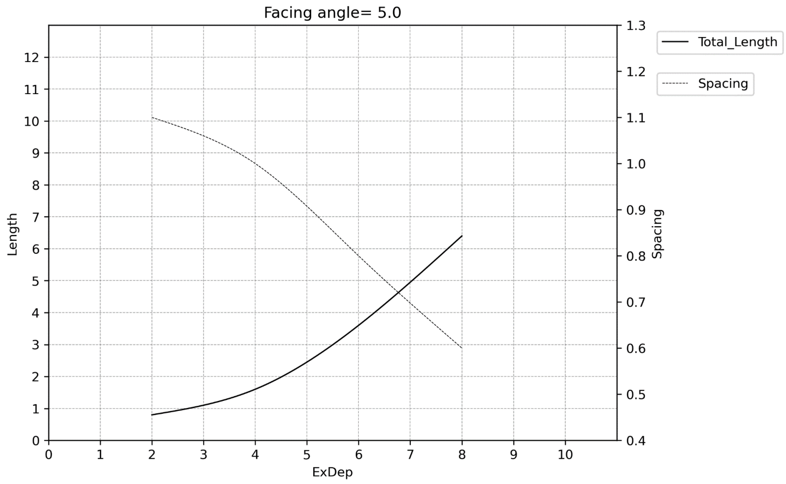

FIGURE 5. For soft slightly plastic loam soil (major quantity: silt, material modelling-Mohr-Coulomb).

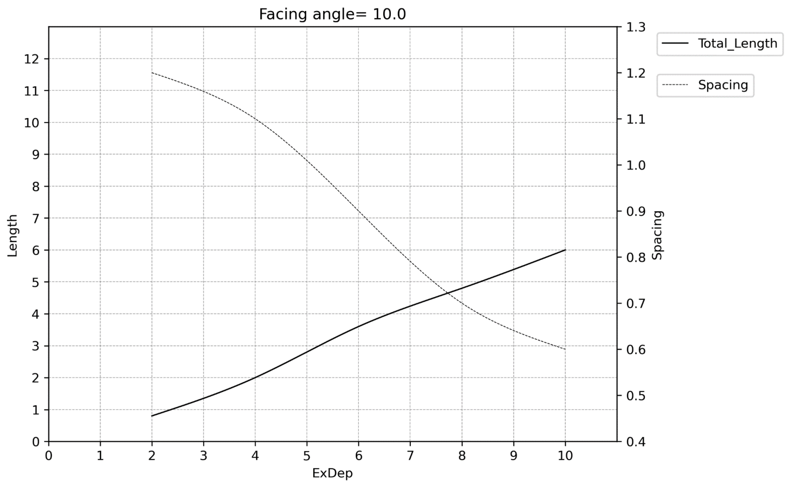

FIGURE 6. For soft slightly plastic loam soil (major quantity: silt, material modelling-Mohr-Coulomb).

30% increase in nail length; (ii) Effect of excavation depth; up to ∼10% FOS decrease and 120% exponential increase in displacement for a 30% increase in depth; (iii) Effect of face angle on FOS (negligible at ±1%) and displacement (maximum of ∼14% reduction with inclination); and (iv) Relative proportions of FOS-based versus displacement-based models. Subsequently, the design charts are presented which serve as an application of the above parametric analysis results.

3.2. **Calibration of Model.** The numerical model of driven soil was calibrated with the help of a reference problem related to stabilized vertical cut using soil nailing from the PLAXIS reference manual [**?**]. In the calibration problem, stabilization of a 6.8 m deep vertical excavation using a soil-nailed wall was carried out for a subway approach under a busy highway in Bangalore, India. This well-known problem was used for the purpose of validating the numerical modeling technique and checking its capability to provide accurate results before carrying out parametric studies. Model validation was done by comparison of the numerical solutions of Factor of Safety

(FOS) against the reference solutions for different cohesion values.

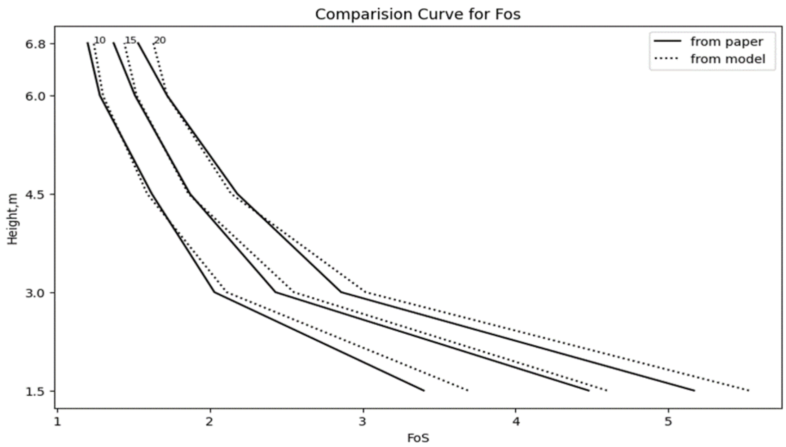

FIGURE 7. Variation of FOS with Excavation Depth (H) between Research Paper and calibrated model.

As can be seen, there was excellent agreement between the numerical results and reference solutions, with average discrepancies of 3.88%, 2.71%, and 4.17% for cohesion values of 10, 15, and 20 kPa, respectively. From this result, it can be concluded that the numerical modeling assumptions, material properties, boundary conditions, and procedures provide accurate results for driven soil-nailed excavation. Thus, the calibrated numerical model was taken as reliable enough to produce a large amount of simulation results. With this calibration model, parametric analysis was done and finding out the parametric relationships. A typical example of parametric relationships can be shown according to Figure 8.

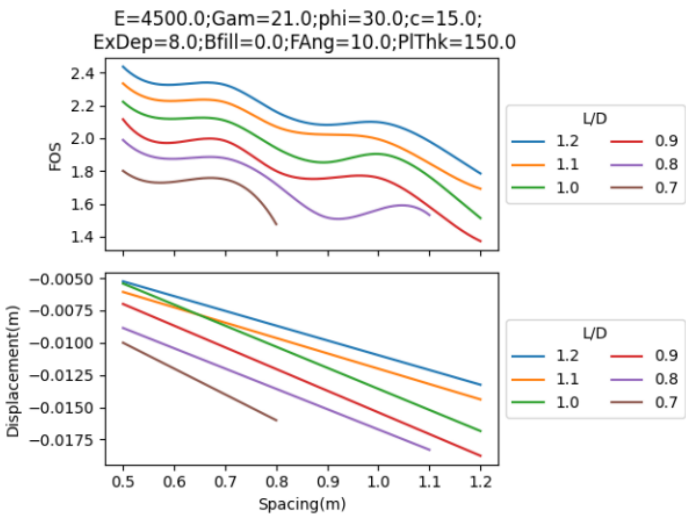

FIGURE 8. Typical example of parametric relationships.

3.3. **Validation of Work.** Figure 9 shows the field tests detail including test models, pull-out test arrangements, inclinometer traversing and a sample plot of inclinometer 2 placed for site 2. The pull-out test performed on the 32 mm diameter soil nail installed demo models (vertical face and 15 degrees inclined slope) at Pulchowk campus shows the satisfactory performance of the structure since it is able to withstand the specified design load of 15 kN (2*DL) to even 24 kN. It can be seen from the data that there exists a stable load-displacement relationship and that the nail gives satisfactory performance even at the end of the test. Particularly, it can be seen that the creep displacement in the last test load is 0.97 mm, which is below the allowed value of 2 mm. This pull-out resistance data was used in FEM modelling in Plaxis.

Based on the inclinometer readings at site 1, there are no signs of any substantial lateral movement in the subsurface soil layer, proving the efficiency of the soil-nailing approach. As seen from the graph, all measurements taken from January through December of 2024 were confined in a vertical range, implying that there have been no tilt and progressive lateral movements during the period of observations. Such results confirm the fact that the soil mass was well restrained and the soil-nailing interaction did not allow for deformations along the direction of the nailing over the whole depth of 6 meters.

Site 1 inclined slope face model of face angle 15 degrees, and Site 2 is vertical face model and nail inclination was 15 degrees in both cases. This field observation and testing results are compatible with numerical results.

From the numerical model, FOS and top displacement are found to be 3.4 and 3.2 mm for site1 and 3.7 and 3.5mm for site 2 respectively. From actual field measurement reading, top displacement for site1 was found to be 3.04 mm, while for site 2 it was found to be 1.31 mm. These values are sufficiently close to consider the model to be verified.

4. CONCLUSION

The comparative study of design charts of the case study presented in Table III for 0.0°, 5.0° and 10.0° of facing angles concludes in the following:

Depth and Slope: Significant rise in facing angles results in increased maximum permissible depth from 6 m to 10 m. The shallow batter lowers the soil pressure thus providing deeper cuts.

Reinforcement Sensitivity: With all other parameters remaining constant, the increase in the depth of excavation requires exponential increase in total length with linear decrease in the spacing. However, facing of 10.0 degree slope provides possibility to increase the density more gradually than a vertical one that requires extremely close spacing of 0.5 m at only 6 m depth.

SSI Effect Optimization: Higher slope causes faster mobilization of stress thus nails should be deeper to go to the failure plane. Increase in the facing angles optimizes the SSI effect and load distribution on the soil nail interface.

Material Efficiency: Although safety factors can be made equal in all the soil types presented in Table III, these figures prove that the geometry of walls is the dominant factor when it comes to material efficiency. The variation of the slope makes it possible for the engineer to reduce nail footage.

By applying this approach to the other soil profiles as shown in Table III (from slightly plastic loam to highly plastic clay), the general conclusions about the scaling capability of the driven soil nails system can be formulated. These general trends show that even though the same safety factor can be achieved in various soils, optimization of the wall geometry is what matters most

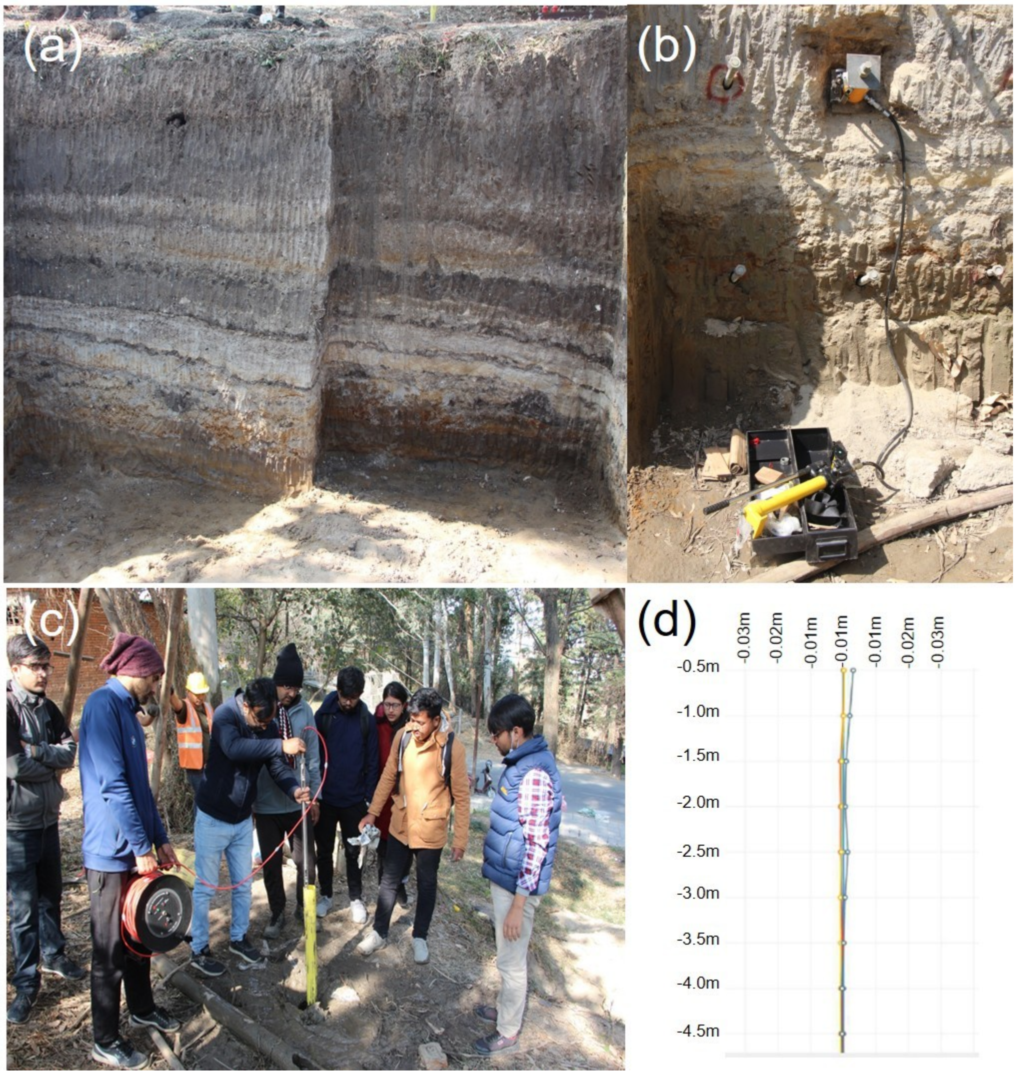

FIGURE 9. Field tests: (a) Test models (vertical, 90 degrees and slope, 85 degrees), (b) Pull-out test with central hole hydraulic jack (nail inclination-15 degrees with horizontal), (c) Inclinometer traversing, (d) Inclinometer profile towards slope direction.

when considering material efficiency. In essence, these results provide the basis for formulating performance based design charts.

Acknowledgment. The authors would like to express their sincere gratitude to the Quality Research and Development Centre (QRDC), Department of Roads (DoR), Government of Nepal for their support and assistance in providing all necessary information and resources to conduct this study. The authors are also grateful to the Research and Training Unit (RTU), Pulchowk Campus, for their support and assistance in conducting this research work.

References

[1] J. Munro, *Introduction to Civil Retaining Structures.* London, UK: Munro Publishing, 2017.
[2] I. Juran, *Design and Construction of Soil Nailed Retaining Structures.* New York, NY, USA: Engineering Press, 1987.

[3] J. A. Porterfield, D. A. Bruce, J. J. Moon, and A. S. Thompson, "Soil nailing field inspectors manual," Federal Highway Administration, Washington, D.C., USA, Tech. Rep. FHWA-SA-93-068, 1994.
[4] Federal Highway Administration, "Soil nail walls reference manual," Federal Highway Administration, Washington, D.C., USA, Tech. Rep., 2015.
[5] P. Patriat and J. Achache, "India–eurasia collision chronology and tectonic implications," *Nature*, vol. 311, pp. 615–621, Oct. 1984.
[6] S. Dhakal, "Geological divisions and hazards in the himalayas," *Journal of Earth Science*, vol. 12, no. 4, pp. 45–58, Mar. 2017.
[7] Y. M. A. Hashash *et al.*, "Major thrust lines and seismic risks," *IEEE Transactions on Geoscience and Remote Sensing*, vol. 53, no. 8, pp. 4200–4215, Aug. 2015.
[8] R. K. Dahal *et al.*, "Geological map and slope stability," Geology Report, Tech. Rep. 98-12, 1998.
[9] National Planning Commission, "The fifteenth plan (2019/20–2022/23)," National Planning Commission, Kathmandu, Nepal, Tech. Rep., 2019.
[10] N. Gurung *et al.*, "Strategic road network planning," Department of Roads, Kathmandu, Nepal, Tech. Rep. SRN-2020, Feb. 2020.
[11] Department of Roads, "Standard specification for road and bridge works," Department of Roads, Kathmandu, Nepal, Tech. Rep., 2016, 2073.
[12] National Reconstruction Authority, "Nepal national building code (nbc)," National Reconstruction Authority, Kathmandu, Nepal, Tech. Rep., 2020.
[13] Plaxis bv, *Plaxis 2D Reference Manual*, Bentley Systems, Exton, PA, USA, 2020.
[14] S. K. Singh and G. L. S. Babu, "Soil nail wall analysis and design: A numerical study," in *Proceedings of Indian Geotechnical Conference*, Mumbai, India, 2010, pp. 455–458.
[15] R. J. Byrne, D. Cotton, J. Porterfield, C. Wolschlag, and G. Mayne, "Checklist and guidelines for review of geotechnical reports and preliminary plans and specifications," Federal Highway Administration, Washington, D.C., USA, Tech. Rep. FHWA-PD-96-001, 1996.